A KIRIGAMI-BASED PARYLENE C STRETCH SENSOR

Alex Baldwin and Ellis Meng
University of Southern California, Los Angeles, USA

ABSTRACT

We present the first slotted Parylene C kirigami device for transducing stretch-induced displacement under multiple modes of operation. Devices consist of thin-film gold traces wound among multiple rows of offset slits etched through a free-film Parylene substrate. Slits were etched via a switched-chemistry DRIE in oxygen plasma, resulting in densely packed slit designs. Multiple slit designs were evaluated and devices with more tightly packed slits were found endure greater stretch distance before failure, with devices containing more tightly packed slits able to stretch up to 9 mm (180%) without plastic deformation or compromise of electrical integrity. Multiple modes of stretch transduction were evaluated, including DC resistance changes due to strain at trace inflection points and high-frequency changes in self-impedance and inter-trace capacitance. DC resistance was found to increase linearly with stretch distance with sensitivities between 0.04 and 0.1 Ω/mm which are comparable to previously reported polyimide sensors but with a wider dynamic measurement range. Capacitance was also found to increase linearly with stretch distance after 2 mm, and high-frequency impedance increased nonlinearly, with different trace routing designs resulting in different patterns of impedance change with stretch.

INTRODUCTION

Kirigami (a Japanese term translating to 'cut' and 'paper') is a technique often used to complement origami and enables creation of three-dimensional shapes from a two-dimensional sheet of paper. By strategically placing cuts in a planar paper substrate and then subjecting the substrate to tension or compression, a huge variety of complex three-dimensional patterns can be produced. Kirigami techniques have been employed in industrial and research applications and proven valuable for producing 3D shapes and actuators in fields ranging from architecture [1] to batteries [2] to biomimetic robots [3]. A common kirigami technique is the use of offset rows of slits to enable a material to stretch far beyond what its normal tensile properties would allow; by converting tensile stress to torsion at specific points between slits, a kirigami slit pattern allows linear movement over a high dynamic range without compromising the structural integrity of the substrate [4]. This effect has been utilized in graphene kirigami devices to achieve stretch distances of up to 267% [5, 6], and on a more flexible Parylene C substrate, tightly packed slits have enabled stretch distances of up to 1100% before tearing occurred [7].

Slotted kirigami devices exhibit minimal material stress in columns between slits, and tensile and compressive stress average to zero along each sliver of material adjacent to a slit, implying stability of electrical connectivity in metal traces wound among these features. However, by introducing non-uniform conduction paths and selectively increasing trace resistance in regions which tend toward either compressive or tensile strain, a trace's DC electrical resistance can correlate with displacement, as seen in previously reported polyimide devices [8]. We developed a stretch device consisting of a thin-film Parylene C substrate with an etched kirigami slit array (Fig. 1). Gold traces were patterned around slits, and both DC and high-frequency properties of these traces were evaluated during stretching with the aim of transducing stretch distance. Previously reported polymer-based stretch sensors exhibited relatively low dynamic ranges and stretch distances that maxed out at around 20% [8, 9]. The combination of flexible, thin-film Parylene with kirigami slit patterns could enable stretch sensors with much higher dynamic ranges.
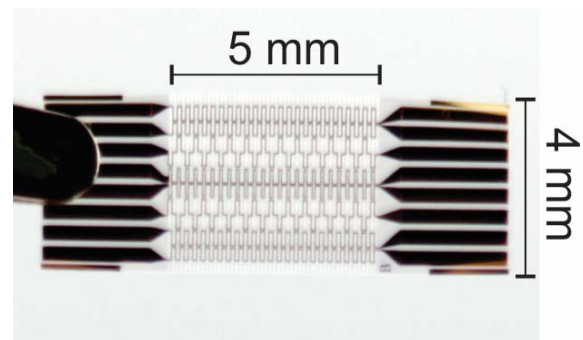

Figure 1: Parylene stretch sensors consist of an actuation section 5 mm long and 4 mm wide containing gold traces wound through an etched kirigami slit array, with two contact pad regions at either end.

DESIGN & FABRICATION

Stretch sensors consisting of gold traces wound among etched slits in a free-standing Parylene substrate were designed and fabricated. Parylene C was chosen as the substrate material due to its high elongation to break (up to 200% [10]), which can lead to higher stretch distances compared to more rigid substrates, and its etchability which allows for placement of precisely aligned, high aspect ratio microscopic slits. Devices contained a slit array over a 5 mm long and 4 mm wide area with two contact pad regions at either end to enable electrical connection and aid in testing.

Two variations of the kirigami slit array were designed. Type A devices contained slits spaced 400 μm apart with inter-row spacing of 200 μm, while type B devices contained slits spaced 150 μm apart in offset rows every 100 μm (Fig. 2). 100 μm was chosen as the smallest separation distance to enable two 20 μm wide gold traces between slits with 20 μm clearance. Both device variations contained slits 600 μm long and 20 μm wide with circular ends 50 μm in diameter to reduce stress. Traces between 5 and 20 μm wide with nominal DC resistance values between 50 and 150 Ω were wound throughout the slit

array. Traces either wound to one side of the slit consistently, to enhance proximity between traces and increase inter-trace capacitance, or alternated sides to isolate self-impedance (Fig. 2B).
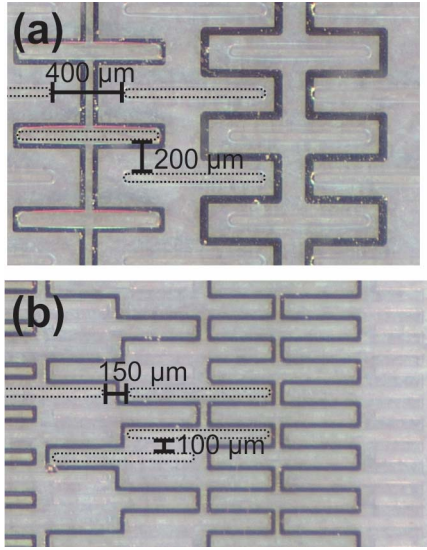

Figure 2: (A) Type A devices contained slits spaced 400 μm apart in offset rows, with 200 μm separation between rows. (B) Type B devices contained slits spaced 150 μm apart in offset rows with 100 μm separation. Traces either wind around slits consistently (right two traces) or alternated sides (right trace).

Fabrication

Fabrication first involved the deposition of 10 μm of Parylene C onto a silicon carrier wafer (Fig. 3). A 200 Å titanium adhesion layer and 2000 Å of gold were then deposited using electron-beam metal deposition and patterned by a liftoff process. A second 10 μm layer of Parylene was deposited as insulation, and the slit array was etched using a switched-chemistry deep reactive ion etch which consisted of alternating etch steps of inductively coupled oxygen plasma and passivation steps of C_4F_8, resulting in an anisotropic etch and slits with high aspect ratios [11]. Contact pads at either end of the device were exposed using a second, lower power deep reactive ion etch to prevent gold sputtering. Devices were released from the silicon carrier wafer by gently peeling while immersed in deionized water.
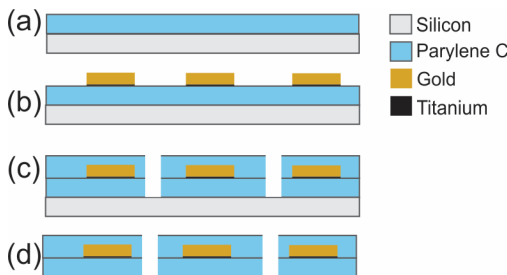

Figure 3: Sensor fabrication involved (a) deposition of Parylene C on a silicon carrier wafer, (b) electron beam deposition and liftoff patterning of 2000 Å Au with 200 Å Ti adhesion layer, (c) etching of slits via a switched-chemistry deep reactive ion etch in oxygen plasma and (d) release from the carrier wafer by peeling while immersed in DI water.

Electrical connection was achieved by attaching a PEEK (polyetheretherketone) backing to contact pads using cyanoacrylate glue and inserting both ends in zero insertion force (ZIF) connectors [12] connected to flat flexible cables (Fig. 4).

Figure 4: Devices were attached to PEEK backing and inserted into ZIF connectors during electrical testing. A stretched device is shown between the ZIF connectors.

Testing Methods

Stretch testing of devices was accomplished by holding one end of the device fixed and stretching the opposing end at a rate of 0.2 mm/s using a ThorLabs moveable stage. DC resistance was measured using a Keithley 2400 SourceMeter and high-frequency impedance and capacitance were measured with an Agilent E4980A LCR meter. Data was collected with a custom LabView program at a rate of 5 Hz.

Three methods of stretch transduction were evaluated. Changes in the DC resistance of a trace monitored changes in strain seen along the conduction path. The high frequency impedance of a single trace measured changes in self-inductance or self-capacitance due to increasing separation of trace sections. The inter-trace capacitance was taken as a measure of net changes in the distance between traces as well as changes in dielectric properties due to the imposed strain on the Parylene substrate.

EXPERIMENTAL RESULTS

Both type A and type B devices were stretched to failure to evaluate the effects of different slit patterns on trace's electrical stability. Stretch distance was defined as the linear displacement from rest of the sensor along the axis between contact pad regions, and percent stretch was defined relative to the length of the slit array (such that 5 mm stretch distance = 100% stretch). DC resistances on type A device traces were stable up to 3.2 mm (64%) of displacement and increased exponentially thereafter until open circuit failure occurred at 3.8 mm (76%), likely due to microcracks in the gold traces at inflection points (Fig. 5). Type B device resistances stayed stable until 6 mm

(120%) of displacement and failed at 9 mm (180%), confirming that increasing slit density enabled greater stretch distances but increased inter-trace width did not improve electrical stability of traces (Fig. 6).
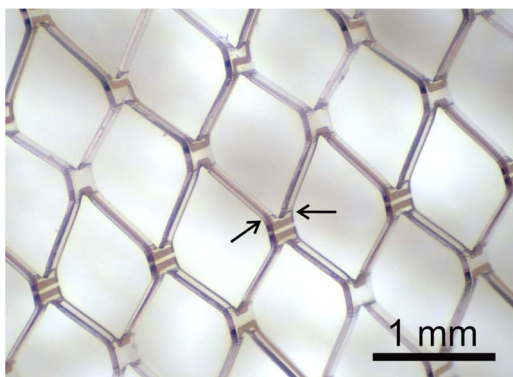

Figure 5: Microscope image of a B type device stretched to 9 mm (180%). Strain is concentrated at two inflection points near the end of the slit.
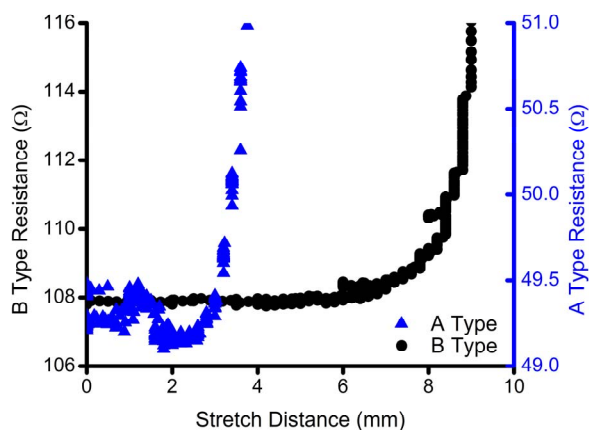

Figure 6: The DC resistance of a trace on A and B type devices stretched at 0.2 mm/s until failure. Tighter slit spacing increased the stretch distance to failure from 76% to 180% and showed that wider spacing between slits did not improve the stability of embedded traces.

Due to the higher achievable stretch distances and stability of electrical traces, B type devices were evaluated for stretch transduction. DC trace resistance was measured during cycling from 0-4 mm displacement, revealing a positive linear correlation between resistance and displacement (sensitivity 0.04-0.1 Ω/mm) (Fig. 7). This stretch sensitivity likely results from increases in strain in the thin-film gold traces, which is concentrated at inflection points near the end of slits. Even without optimization, the sensitivity of resistance-based stretch transduction was competitive with previously reported polyimide devices, with Parylene devices possessing a higher dynamic range even within a conservative testing protocol (0.09 Ω/mm over 80% displacement vs -0.18 Ω/mm over 20% displacement in polyamide devices [6]).

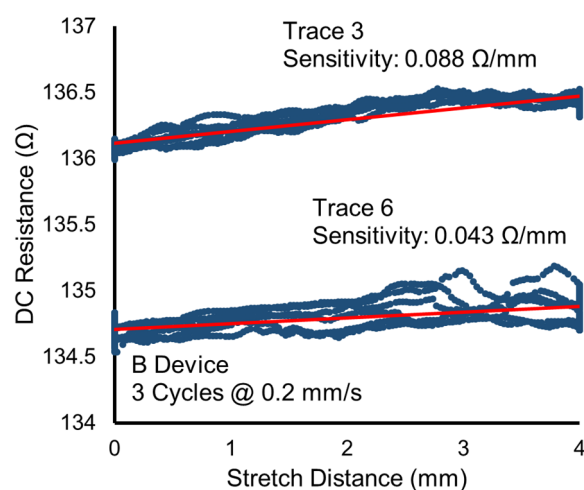*Figure 7: The DC resistance of alternating traces on a B device over multiple stretch cycles, showing sensitivities of 0.043 and 0.088 /mm. Both traces are of the same design; differences in baseline resistance are likely due to process variations.*

Capacitance between adjacent consistently-wound traces was evaluated at 100 kHz. Capacitance was found to be relatively stable up to 2 mm displacement and to increase linearly at a rate of 4.7 fF/mm between 2 and 5 mm displacement (Fig. 8). Such changes in capacitance may result from net changes in separation distance between traces or changes in the dielectric constant of Parylene induced by stress.
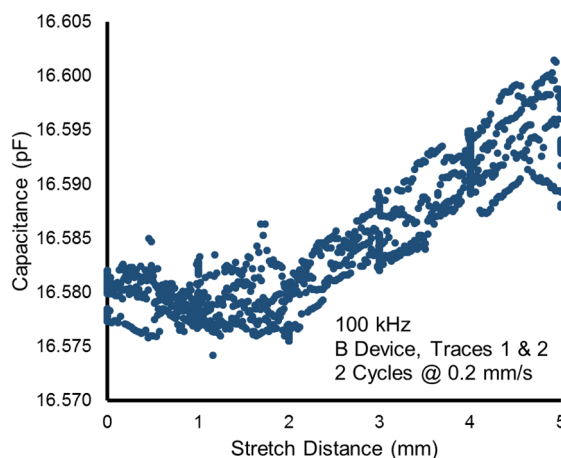

Figure 8: The capacitance between two adjacent traces in a B device, measured at 100 kHz. At around 2 mm displacement, the capacitance begins to increase linearly with stretch distance.

Complex impedance at 2 MHz was recorded for a single trace during stretching from 0-5 mm. Impedance magnitude showed a nonlinear dependence with stretch distance which varied depending on whether traces wound to one side of slits consistently or alternated winding side. Consistent traces showed a sigmoidal increase in impedance with an inflection point at approximately 2.5 mm displacement and a total resistance change between 0 and 5 mm of displacement of about 1%, while alternating

traces showed a simpler curved trend and a total resistance change of around 0.4% (Fig. 9).
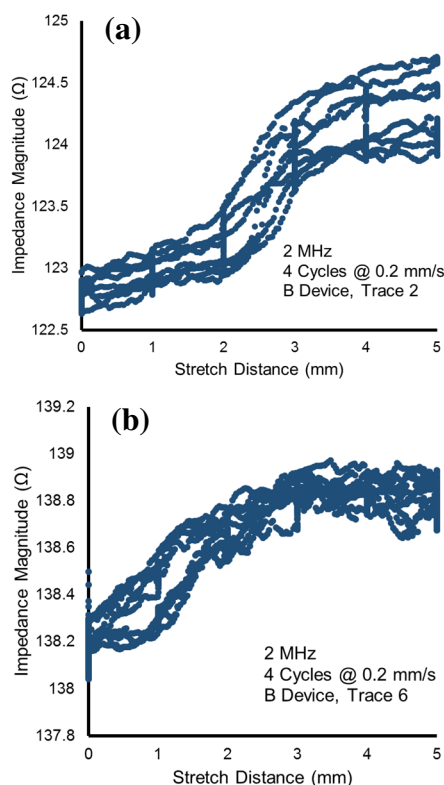

Figure 9: The high-frequency impedance magnitude shows a non-linear relationship with stretch distance, with (A) a sigmoidal relationship for consistent traces and (B) a curved relationship for alternating traces.

DISCUSSION & FUTURE WORK

Kirigami devices constructed of Parylene and gold were fabricated and found to have multiple electrical parameters which vary predictably with stretch distance. DC resistance's sensitivity to stretch distance was found to be of comparable sensitivity to previously reported polymer sensors but with a higher dynamic range and simpler trace geometry. Inter-trace capacitance and high-frequency inductance also varied with stretch distance, which could lead to additional sensing modalities based off of frequency transduction as opposed to resistive transduction.

Construction out of only Parylene and gold renders these sensors not only resistant to corrosion but fully biocompatible and suitable for chronic implantation in the human body. This contrasts with other common strain sensors which utilize semiconductor-based piezoresistive materials or carbon nanotubes for stretch sensing, neither of which is able to be chronically implanted. A high dynamic range, low strain stretch sensor could potentially be used in numerous biomedical applications, such as monitoring bladder size for the treatment of urinary incontinence, sensing muscle stretch for improved proprioception, or integrating with fabric-based wearables for non-invasive movement transduction.

Future work will involve optimizing slit size and orientation in order to maximize stretch distance and minimize internal stress, as well as exploring different trace geometries which may improve stretch sensitivity. Capacitive and impedance-based stretch transduction will also be further explored with the goal of developing sensors which transduce stretch via changes in resonant frequency instead of resistance. The attachment of a Parylene-based coil would render such systems wireless and fully implantable.

REFERENCES

1. Weston, M., *Anisotropic Operations.* International Journal of Architectural Computing, 2012. **10**(1): p. 105-120.
2. Song, Z., et al., *Kirigami-based stretchable lithium-ion batteries.* Scientific reports, 2015. **5**.
3. Sareh, S. and J. Rossiter, *Kirigami artificial muscles with complex biologically inspired morphologies.* Smart Materials and Structures, 2012. **22**(1): p. 014004.
4. Kotov, N.A., et al., *Kirigami Nanocomposites as Wide-Angle Diffraction Gratings.* ACS nano, 2016.
5. Blees, M.K., et al., *Graphene kirigami.* Nature, 2015.
6. Shyu, T.C., et al., *A kirigami approach to engineering elasticity in nanocomposites through patterned defects.* Nature materials, 2015.
7. Morikawa, Y., et al. *An origami-inspired ultrastretchable bioprobe film device.* in *2016 IEEE 29th International Conference on Micro Electro Mechanical Systems (MEMS).* 2016. IEEE.
8. Firouzeh, A. and J. Paik, *The design and modeling of a novel resistive stretch sensor with tunable sensitivity.* IEEE Sensors Journal, 2015. **15**(11): p. 6390-6398.
9. Lee, C., L. Jug, and E. Meng, *High strain biocompatible polydimethylsiloxane-based conductive graphene and multiwalled carbon nanotube nanocomposite strain sensors.* Applied Physics Letters, 2013. **102**(18): p. 183511.
10. Kim, B.J. and E. Meng, *Micromachining of Parylene C for bioMEMS.* Polymers for Advanced Technologies, 2015.
11. Meng, E., P.-Y. Li, and Y.-C. Tai, *Plasma removal of Parylene C.* Journal of Micromechanics and Microengineering, 2008. **18**(4): p. 045004.
12. Gutierrez, C.A., et al. *Epoxy-less packaging methods for electrical contact to parylene-based flat flexible cables.* in *2011 16th International Solid-State Sensors, Actuators and Microsystems Conference.* 2011. IEEE.